Institute of Physics Publishing
doi:10.1088/1742-6596/4/1/044
Journal of Physics: Conference Series **4** (2005) 286–289
Sixth International Conference on Dissociative Recombination

Position- and time-sensitive coincident detection of fragments from the dissociative recombination of O_2^+ using a single hexanode delay-line detector

F Österdahl,[1] S Rosén,[2] V Bednarska,[2] A Petrignani,[3] F Hellberg,[4] M Larsson[4] and W J van der Zande[2]

[1]Department of Physics, Royal Institute of Technology, AlbaNova University Centre, SE 106 91 Stockholm, Sweden
[2]Molecule and Laser Physics, IMM, Radboud University Nijmegen, Toernooiveld 1, 6525 ED Nijmegen, The Netherlands
[3]FOM Institute for Atomic and Molecular Physics, Kruislaan 407, 1098 SJ, Amsterdam, The Netherlands
[4]Molecular Physics, Stockholm University, Albanova University Centre, SE 106 91 Stockholm, Sweden

E-mail: wim.vanderzande@science.ru.nl

Abstract. This contribution describes the use of the RoentDek hexanode delay line detector to detect fragments from the dissociative recombination of O_2^+ in an experiment at the ion storage ring CRYRING, Manne Siegbahn Laboratory, Stockholm. In this experiment, the fragments have a maximum time- and position-separation of 20 ns and 40 mm, respectively. The position resolution obtained was 0.16 mm (FWHM) on the 67 mm diameter detector. The time resolution obtained from the time-of-arrival difference between the product fragments was about 1 ns. The detector system handles event rates as large as 30 kHz. Techniques for the calibration of the absolute position of particles on the detector are discussed.

We have used the RoentDek hexanode delay line detector (DLD) to extract product state information in the dissociative recombination (DR) of O_2^+ in the heavy ion storage ring CRYRING in Stockholm. DR experiments aimed at obtaining product state information place a series of specific demands on detectors which are often hard to meet. Product state information is obtained by retrieving the kinetic energy released, in individual DR reactions, from the time- and position detection of all the product fragments. The use of fast ion beams facilitates detection of all the fragments on a single detector. The high beam energies (MeV) in a storage ring, in comparison with the few eV of kinetic energy released in the DR reaction, demands a large distance from the interaction region to the detector and still results in small time separations between the fragments. A detector is therefore needed having both high time- and spatial-resolution. The experimental condition dictates that all of the reaction fragments need to be detected and hence requires a detector system that analyzes event per event. The hexanode DLD meets nearly all of these requirements. The principles behind its operation can be found in the literature [1] and some of the most important aspects of relevance here will be described in the following.

The incoming fragments hit a pair of microchannel plates (MCP), making clouds of electrons which are picked up by three layers of anode delay-line (DL) wires, arranged at an angle of 60 degrees with respect to each other. The position along one DL for an incoming particle is described by $u_i = (t_i^{(1)} - t_i^{(2)})/2v_i$, with the origin defined in the center of the DL, and where $t_i^{(1)}$ and $t_i^{(2)}$ are the travel times to each DL-end, respectively; v_i is the propagation speed of the signal along the DL, and $i = 1$–3 represents each of the three DLs. The use of three DLs instead of two (x,y), ensures the presence

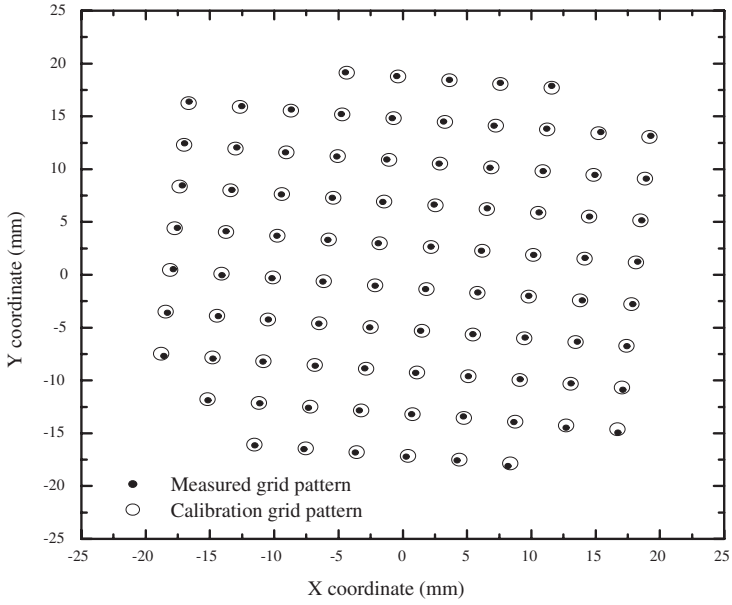

Figure 1. The calibration grid (open circles) has 0.2 mm holes in a 4×4 mm grid pattern. The solid dots are the measured pattern.

of redundant information that can be used to disentangle the data of two coincident fragments. The hexanode DLD gives the positions and the difference in time-of-arrival between the two fragments for each DR event.

To calibrate the propagation speed of the signal along each DL, a grid was placed in front of the detector. The calibration grid, along with the measured grid pattern, are shown in figure 1. The error in position between the calibration grid and the measured grid is 0.16 mm (FWHM). Figure 2 shows the time sum, which is defined as $T^{\mathrm{sum}}_{i,a} = (t^{(1)}_i + t^{(2)}_i)$, for each first hit, a, and is always constant. The second arriving fragment, b, will have a time sum which is $T^{\mathrm{sum}}_{i,b} = T^{\mathrm{sum}}_{i,a} + 2\,ToA$, where ToA is the arrival time difference between the fragments. In the study on the DR of O_2^+ the total ion beam energy used was 1 MeV and the distance from the center of the interaction region to the DLD was about 8 m. The space and time separation of the fragments for the different atomic limits under these conditions are shown in table 1.

Figure 3 shows the distance distribution for the DR of O_2^+ where the parent ions are mainly populated in the lowest vibrational level (90.3 % in $v = 0$). The distances here are the projection of the total

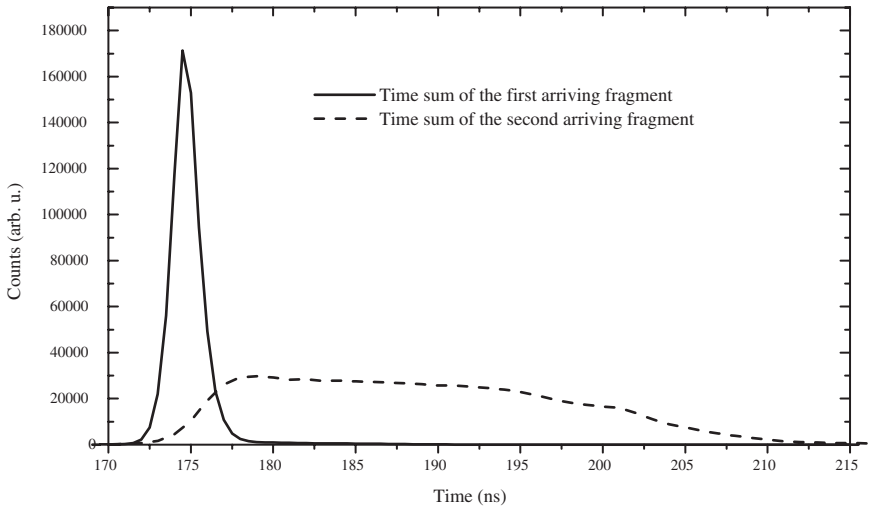

Figure 2. Shows that the time sums contain arrival time information. See text for details.

Table 1. The maximum spatial and time separations between the two fragments for the different dissociation limits

	Atomic limit	Max. Time Separation (ns)	Max. Spatial Separation (mm)
$O_2^+(X^2\Pi_g, v=0) + e^- \rightarrow$	$O(^3P) + O(^3P) + 6.95$ eV	18	43
	$O(^3P) + O(^1D) + 4.99$ eV	15	37
	$O(^1D) + O(^1D) + 3.02$ eV	12	29
	$O(^1D) + O(^1S) + 0.80$ eV	6	15

separation of the two O fragments on the plane of the detector. The DLD data (broken line) are compared with the 2D data from Petrignani *et al.* [2] (open circles, both the *x*- and *y*-axis have been scaled to fit the DLD data) and also with a Monte Carlo simulation of the reaction (solid line). The data obtained by Petrignani *et al.* were measured using a CCD camera set-up [3]. Differences in the compared data are observed, and can be explained by the following effects. In the experiment using the DLD, some reduction of efficiency occurs near the largest KER values because of the size of the ion beam and the size of the detector. Another, relatively small, effect can be observed in the peak-widths that arise from the different vibrational populations of the ion beam. At small distances there is also a large difference, and this will be discussed next.

The main advantages of the DLD should be mentioned and can be appreciated from figure 3. The count rate of the DLD detector is very high, and can be above 30 kHz. The spatial resolution of the DLD is also high and the bin size is 0.1 mm. The data obtained from the much slower CCD camera set-up [3] are binned in 1 mm intervals. The main disadvantage is the occurrence of a significant "dead area" that obscures small distance events. This area is due to the dead time of the electronics, in particular the constant fraction discriminator (CFD) and the time-to-digital converters (TDC) used. The analysis procedure makes use of a general "sorter routine" which considers the DL data as coming from a many-fragment event. In the DR of O_2^+ only two fragments appear, which enables us to still record in the 2D distance range of ~ 4 to ~ 13 mm; however, the efficiency is reduced to an estimated value of $\sim 25\%$ below 13 mm. Unfortunately, only a limited number of small distance events could be retrieved. The simulation of the reaction, shown in figure 3 (solid line), demonstrates the significance of the deviation between the simulation and the DLD data (broken line). In the present experiment no information could be retrieved from the lowest kinetic energy DR channel (see table 1). The parameters in the simulation are

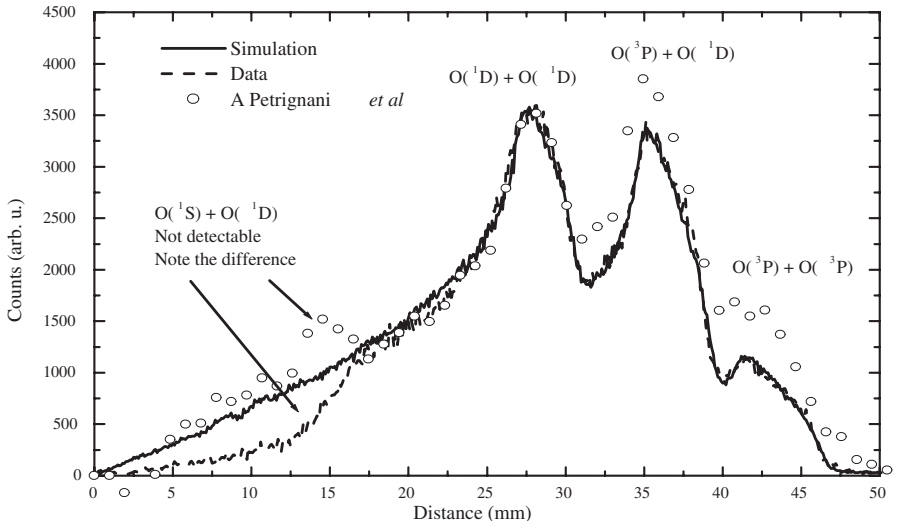

Figure 3. 2D distance distribution.

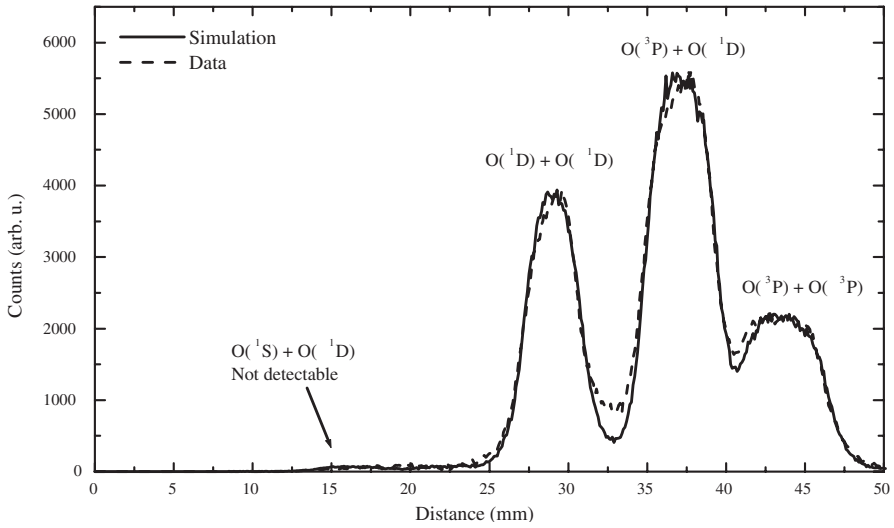

Figure 4. 3D distance distribution.

the detector parameters, for example the position- and time-resolution of the detector, and the ion beam parameters, such as vibrational and rotational temperature, as well as the branching over the different channels [2].

Figure 4 shows the resolved 3D distances between the fragments (broken line). These 3D data are retrieved from the measured distance in the plane of the DLD and the measured difference in time-of-arrival and hence give the resolved 3D distribution. It is remarkable how well the different dissociation channels are separated now. The spectra show a clear separation between the different kinetic energies. The data are plotted in mm for convenience. However, they are also proportional to the square root of the kinetic energy release, hence the 3D data represent a direct measurement of the kinetic energy release in the reaction. The smallest kinetic energy channel is still, however, not measurable. A Monte Carlo simulation for the 3D spectra (solid line), similar to that of the 2D spectra, is carried out and compared with the data. These 3D data will provide much more accurate branching fractions than the 2D spectra used until now.

The high resolution, both spatial and temporal, and the high count rate make it possible to achieve more detailed studies on the dynamics of the DR reaction. The high count rate of the DLD increases the overall efficiency for detectors used in DR experiments. Future improvements could be possible by minimizing the "dead area"; the CFD in combination with the TDC could be replaced by a fast digitizer in order to enable software manipulation of the DL signals.

Acknowledgments

This work is part of the research program of the "Stichting voor Fundamenteel Onderzoek der Materie (FOM)", which is financially supported by the "Nederlandse organisatie voor Wetenschappelijk Onderzoek (NWO)". Support has also been given by the EU research-training network Electron Transfer Reactions (ETR) under HPRN-CT-2000-00142. We thank the staff of the Manne Siegbahn Laboratory for their part in making the experiments possible.

References

[1] Jagutzki O *et al.* 2002 *IEEE Transact. on Nucl. Science* **49** 2477
[2] Petrignani A, Cosby P C, Hellberg F, Thomas R D, Larsson M and van der Zande W J 2004 *J. Chem. Phys.* in press
[3] Hellberg F *et al.* 2003 *J. Chem. Phys.* **118** 6250